JOURNAL OF MULTIFUNCTIONAL MATERIALS & PHOTOSCIENCE
12(2), December 2021, pp. 173-181

Synthesis and Spectroscopic properties of Microcrystalline $NaCaLa(WO_4)_3$:Ho^{3+}/Yb^{3+} Upconversion Yellow Phosphors

Won-Chun Oh, Zambaga Otgonbayar, Md Nazmodduha Rafat, Kamrun Nahar Fatema, Chang Sung Lim

Department of Aerospace Advanced Materials & Chemical Engineering, Hanseo University, Seosan 31962, Republic of Korea

Abstract: Microcrystalline Ho^{3+}/Yb^{3+} co-doped $NaCaLa_{1-x}(WO_4)_3$ yellow phosphors were successfully synthesized with variations of Ho^{3+} and Yb^{3+} (x = Ho^{3+} + Yb^{3+}, Ho^{3+} = 0.05, 0.1, 0.2 and Yb^{3+} = 0.2, 0.45), and their upconversion (UC) photoluminescence (PL) properties were evaluated. The synthesized particles have been fairly crystallized and showed a superior microcrystalline morphology with particle sizes of 5-10 ìm. The spectroscopic properties were examined comparatively using PL emission and Raman spectroscopy. Under excitation at 980 nm, the UC intensities of $NaCaLa_{0.5}(WO_4)_3$: $Ho_{0.05}Yb_{0.45}$ particles exhibited yellow emissions based on a strong 550-nm emission band in the green region and a very strong 655-nm emission band in the red region; these emissions were assigned to the $^5S_2/^5F_4 \rightarrow {}^5I_8$ and $^5F_5 \rightarrow {}^5I_8$ transitions, respectively. The pump power dependence was provided, and the Raman spectra of the doped particles indicated the domination of strong peaks induced by the disorder of the $[WO_4]^{2-}$ groups with the incorporation of the Ho^{3+} and Yb^{3+} elements into the crystal lattice or by a new phase formation.

Keywords: Microcrystalline, Yellow Phosphors, Upconversion, Spectroscopic, Raman

1. Introduction

Rare-earth activated upconversion (UC) materials have been widely applied in the fields, such as lighting sources, display terminals, and biological detectors [1]. Such materials offer potential for numerous advantages in analytical applications in comparison to molecular fluorophores and quantum dots. In order to overcome the current limitations in traditional photoluminescence materials, the synthesis and characterization of UC particles have attracted considerable interest since they are considered as potentially active components in new optoelectronic devices and luminescent products [2, 3]. Almost lanthanide doped $MR(WO_4)_2$ have a tetragonal scheelite structure with the space group $I4_{1/a}$, and belong to the family of double tungstate compounds. For the trivalent lanthanide ions in the disordered tetragonal-phase it is possible to be partially substituted by Ho^{3+} and Yb^{3+} ions. Because of the similar radii of the trivalent lanthanide ions, these

* Corresponding author: *E-mail: cslim@hanseo.ac.kr*

ions are effectively doped into the crystal lattices of the tetragonal phase in high red emitting efficiency under superior thermal and chemical stability. In the crystal structure, W^{6+} is coordinated by four O^{2-} at a tetrahedral site, which makes $[WO_4]^{2-}$ relatively stable [4-6]. The $[WO_4]^{2-}$ group has strong absorption in the near ultraviolet region, so that energy transfers process from $[WO_4]^{2-}$ group to rare earth ions can easily occur, which can greatly enhance the external quantum efficiency of rare earth ions doped materials.

Among rare-earth ions, the Ho^{3+} ion is suitable for converting infrared to visible light through the UC process due to its appropriate electronic energy level configuration. Co-doped Yb^{3+} ion and Ho^{3+} ion can remarkably enhance the UC efficiency for the shift from infrared to visible light due to the efficiency of the energy transfer from Yb^{3+} to Ho^{3+}. The Yb^{3+} ion, as a sensitizer, can be effectively excited by an incident light source energy. This energy is transferred to the activator from which radiation can be emitted. The Ho^{3+} ion activator is the luminescence center of the UC particles, while the sensitizer Yb^{3+} enhances the UC luminescence efficiency [7-9].

Several processes have been developed for specific purposes to prepare these rare-earth doped double tungsates [10-16]. Compared with the usual methods, microwave synthesis has the advantages of a very short reaction time, small-size particles, narrow particle size distribution, and high purity of final polycrystalline samples. Microwave heating is delivered to the material surface by radiant and/or convection heating, which heat energy is transferred to the bulk of the material via conduction. However, synthesis of $NaCaLa(WO_4)_3$:Ho^{3+}/Yb^3 yellow phosphors by the cyclic microwave-modified sol-gel method has not yet been reported.

In this study, $NaCaLa_{1-x}(WO_4)_3$:Ho^{3+}/Yb^{3+} phosphors with doping concentrations of Ho^{3+} and Yb^{3+} (x = Ho^{3+} + Yb^{3+}, Ho^{3+} = 0.05, 0.1, 0.2 and Yb^{3+} = 0.2, 0.45) were prepared by cyclic the microwave-modified sol-gel method followed by heat treatment. The synthesized particles were characterized by X-ray diffraction (XRD), scanning electron microscopy (SEM), and energy-dispersive X-ray spectroscopy (EDS). The optical properties were examined comparatively using photoluminescence (PL) emission and Raman spectroscopy.

Experimental

Appropriate stoichiometric amounts of $Na_2WO_4 \cdot 2H_2O$ (99%, Sigma-Aldrich, USA), $Ca(NO_3)_2 \cdot 4H_2O$ (99%, Sigma-Aldrich, USA), $La(NO_3)_3 \cdot 6H_2O$ (99%, Sigma-Aldrich, USA), $(NH_4)_6W_{12}O_{39} \cdot xH_2O$ (99%, Alfa Aesar, USA), $Ho(NO_3)_3 \cdot 5H_2O$ (99.9%, Sigma-Aldrich, USA), $Yb(NO_3)_3 \cdot 5H_2O$ (99.9%, Sigma-Aldrich, USA), citric acid (99.5%, Daejung Chemicals, Korea), NH_4OH (A.R.), ethylene glycol (A.R.) and distilled water were used to prepare $NaCaLa(WO_4)_3$, $NaCaLa_{0.8}(WO_4)_3$:$Ho_{0.2}$, $NaCaLa_{0.7}(WO_4)_3$:$Ho_{0.1}Yb_{0.2}$, and $NaCaLa_{0.5}(WO_4)_3$:$Ho_{0.05}Yb_{0.45}$ compounds with doping concentrations of Ho^{3+} and Yb^{3+} (Ho^{3+} = 0.05, 0.1, 0.2 and Yb^{3+}= 0.2, 0.45). To prepare $NaCaLa(WO_4)_3$, 0.2 mol% $Na_2WO_4 \cdot 2H_2O$ and 0.083 mol% $(NH_4)_6W_{12}O_{39} \cdot xH_2O$ were dissolved in 20 mL of ethylene

glycol and 80 mL of 5M NH_4OH under vigorous stirring and heating. Subsequently, 0.4 mol% $Sr(NO_3)_3$ and citric acid (with a molar ratio of citric acid to total metal ions of 2:1) were dissolved in 100 mL of distilled water under vigorous stirring and heating. Then, the solutions were mixed together under vigorous stirring and heating at 80-100°C. Finally, highly transparent solutions were obtained and adjusted to pH=7-8 by the addition of NH_4OH or citric acid. In order to prepare $NaCaLa_{0.8}(WO_4)_3:Ho_{0.2}$, the mixture of 0.32 mol% $La(NO_3)_3 \cdot 6H_2O$ with 0.08 mol% $Ho(NO_3)_3 \cdot 5H_2O$ was used for the creation of the rare earth solution. In order to prepare $NaCaLa_{0.7}(WO_4)_2:Ho_{0.1}Yb_{0.2}$, the mixture of 0.28 mol% $La(NO_3)_3 \cdot 6H_2O$ with 0.04 mol% $Ho(NO_3)_3 \cdot 5H_2O$ and 0.08 mol% $Yb(NO_3)_3 \cdot 5H_2O$ was used for the creation of the rare earth solution. In order to prepare $NaCaLa_{0.5}(WO_4)_3:Ho_{0.05}Yb_{0.45}$, the rare earth containing solution was generated using 0.2 mol% $La(NO_3)_3 \cdot 6H_2O$ with 0.02 mol% $Ho(NO_3)_3 \cdot 5H_2O$ and 0.18 mol% $Yb(NO_3)_3 \cdot 5H_2O$.

The transparent solutions were placed for 30 min into a microwave oven operating at a frequency of 2.45 GHz with a maximum output-power of 1250 W. The working cycle of the microwave reaction was controlled very precisely using a regime of 40 s on and 20 s off for 15 min, followed by further treatment of 30 s on and 30 s off for 15 min. The ethylene glycol was evaporated slowly at its boiling point. Ethylene glycol is a polar solvent at its boiling point of 197°C, this solvent is a good candidate for the microwave process. The charged particles vibrate in the electric field interdependently when a large amount of microwave radiation is supplied to the ethylene glycol. The samples were treated with ultrasonic radiation for 10 min to produce a light yellow transparent sol. After this, the light yellow transparent sols were dried at 120°C in a dry oven to obtain black dried gels. The black dried gels were grinded and heat-treated at 850°C for 16 h with 100°C intervals between 600-900°C. Finally, white particles were obtained for $NaCaLa(WO_4)_3$ and pink particles were obtained for the doped compositions.

The phase composition of the synthesized particles was identified using XRD (D/MAX 2200, Rigaku, Japan). The microstructure and surface morphology of the synthesized particles were observed using SEM/EDS (JSM-5600, JEOL, Japan). The PL spectra were recorded using a spectrophotometer (Perkin Elmer LS55, UK) at room temperature. Raman spectroscopy measurements were performed using a LabRam Aramis (Horiba Jobin-Yvon, France). The 514.5-nm line of an Ar ion laser was used as the excitation source; the power on the samples was kept at 0.5 mW.

Results and Discussion

Fig. 1 shows the X-ray diffraction patterns of the (a) JCPDS 41-1431 data of $CaWO_4$, and the synthesized (b) $NaCaLa(WO_4)_3$, (c) $NaCaLa_{0.8}(WO_4)_3:Ho_{0.2}$, and (d) $NaCaLa_{0.7}(WO_4)_3:Ho_{0.1}Yb_{0.2}$, and (e) $NaCaLa_{0.5}(WO_4)_3:Ho_{0.05}Yb_{0.45}$ particles. The diffraction patterns of the products can be mostly consistent with the standard data of $CaWO_4$ (JCPDS 41-1431). No impurity phases were detected. $NaCaLa(WO_4)_3$ as a member of double tungstate family has a scheelite structure which is tetragonal with a space group $I4_{1/a}$ [11]. In $NaCaLa(WO_4)_3$ matrix, Na^+ and La^{3+} are randomly arranged and form

a disordered structure. Ho^{3+} and Yb^{3+} ions can be effectively doped in the $NaCaLa(WO_4)_3$ lattice by partial substitution of La^{3+} site due to the similar radii of La^{3+}, Ho^{3+} and Yb^{3+}, form an identical S_4 local symmetry. Post heat-treatment plays an important role in a well-defined crystallized morphology. To achieve a well-defined crystalline morphology, the phases need to be heat treated at 850°C for 16 h. It is assumed that the doping amount of Ho^{3+}/Yb^{3+} has a great effect on the crystalline cell volume of the $NaCaLa(WO_4)_3$, because of the different ionic sizes and energy band gaps. It is assumed that the doping amount of $Ho^{3+}+Tm^{3+}/Yb^{3+}$ has a great effect on the crystalline cell volume of the NCLW, because of the different ionic sizes of the substitution of Ho^{3+} (R=1.015 Å) and Yb^{3+} (R=0.985 Å) ions in the La^{3+} (R=1.16 Å) sites [17].

Fig. 1: X-ray diffraction patterns of the (a) JCPDS 41-1431 data of $CaWO_4$, the synthesized (b) $NaCaLa(WO_4)_3$, (c) $NaCaLa_{0.8}(WO_4)_3:Ho_{0.2}$, (d) $NaCaLa_{0.7}(WO_4)_3:Ho_{0.1}Yb_{0.2}$, and (e) $NaCaLa_{0.5}(WO_4)_3:Ho_{0.05}Yb_{0.45}$ particles.

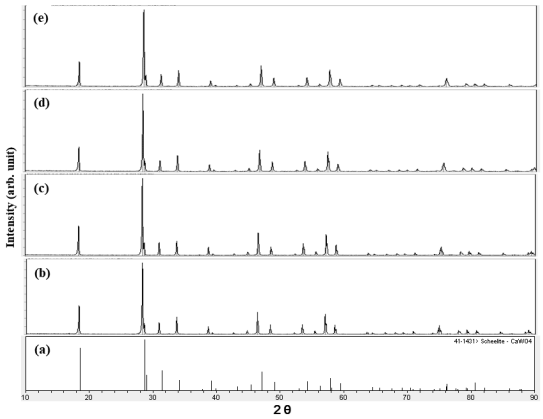

Fig. 2 shows a SEM image of the synthesized $NaCaLa_{0.5}(WO_4)_3:Ho_{0.05}Yb_{0.45}$ particles. The as-synthesized sample is well crystallized with a fine and homogeneous morphology and particle size of 5-10 ìm. It is noted that the structure has a tetragonal–phase after partial substitution of La^{3+} by Ho^{3+} and Yb^{3+} ions, and the ions are effectively doped into crystal lattices of the $NaCaLa(WO_4)_3$ phase.

Fig. 2: Scanning electron microscopy image of the synthesized $NaCaLa_{0.5}(WO_4)_3:Ho_{0.05}Yb_{0.45}$ particles.

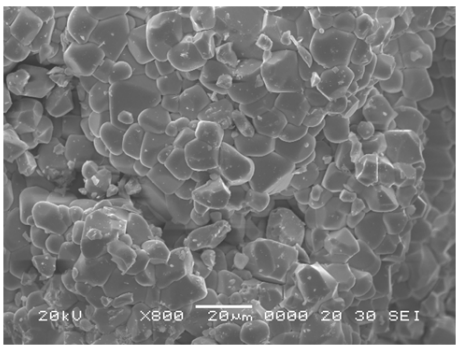

Fig. 3 shows the (a) energy-dispersive X-ray spectroscopy patterns, (b) quantitative compositions and (c) quantitative results of the synthesized $NaCaLa_{0.7}(WO_4)_3$: $Ho_{0.1}Yb_{0.2}$particles. The EDS pattern (a) shows that the $NaCaLa_{0.7}(WO_4)_3$: $Ho_{0.1}Yb_{0.2}$ particles are composed of Na, Ca, La, Mo, O, Ho and Yb. The quantitative compositions (b) show precise constitutions of the synthesized $NaCaLa_{0.7}(WO_4)_3$:$Ho_{0.1}Yb_{0.2}$ particles. The quantitative results (c) are in good relation with a nominal composition of the $NaCaLa_{0.7}(WO_4)_3$:$Ho_{0.1}Yb_{0.2}$ particles. The relations between Na, Ca, La, Mo, O, Ho and Yb show that the $NaCaLa_{0.7}(WO_4)_3$:$Ho_{0.1}Yb_{0.2}$ particles can be successfully synthesized using the cyclic microwave-assisted sol-gel method. The cyclic microwave-assisted sol-gel process of tungstate provides the energy to synthesize the bulk of the material uniformly, so that fine particles with controlled morphology can be fabricated in a short time period. The method is a cost-effective way to provide highly homogeneous products and is easy to scale-up, it is a viable alternative for the rapid synthesis of UC particles.

Fig. 3: Energy-dispersive X-ray spectroscopy patterns (a), quantitative compositions (b) and quantitative results (c) of the synthesized $NaCaLa_{0.7}(WO_4)_3$:$Ho_{0.1}Yb_{0.2}$ particles.

(a)

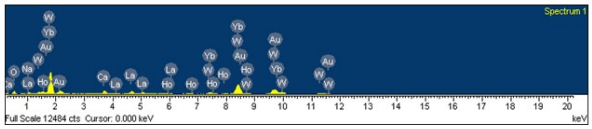

(b)

Spectrum	In stats.	O	Na	Ca	La	Ho	Yb	W	Au	Total
Spectrum 1	Yes	20.18	1.71	3.61	10.66	3.49	7.20	43.51	9.64	100.00
Spectrum 2	Yes	20.28	1.80	3.45	10.60	3.46	7.14	43.93	9.33	100.00
Spectrum3	Yes	20.27	1.79	3.52	10.37	3.81	8.01	43.14	9.09	100.00
Mean		20.25	1.77	3.53	10.54	3.59	7.45	43.53	9.36	100.00
Std. deviation		0.06	0.05	0.08	0.15	0.20	0.48	0.40	0.27	
Max.		20.28	1.80	3.61	10.66	3.81	8.01	43.93	9.64	
Min.		20.18	1.71	3.45	10.37	3.46	7.14	43.14	9.09	

(c)

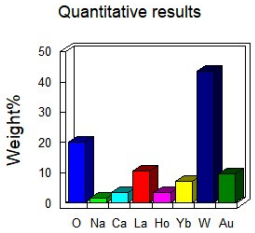

Fig. 4 shows the UC photoluminescence emission spectra of the as-prepared (a) $NaCaLa(WO_4)_3$, (b) $NaCaLa_{0.8}(WO_4)_3$:$Ho_{0.2}$, (c) $NaCaLa_{0.7}(WO_4)_3$:$Ho_{0.1}Yb_{0.2}$, and (d) $NaCaLa_{0.5}(WO_4)_3$:$Ho_{0.05}Yb_{0.45}$ particles excited under 980 nm at room temperature. The highest UC intensities of (d) $NacaLa_{0.5}(WO_4)_3$:$Ho_{0.05}Yb_{0.45}$ particles exhibited yellow emissions based on a strong 550-nm emission band in the green region and a very strong 655-nm emission band in the red region. The UC intensities of (a) $NaCaLa(WO_4)_3$ and (b) $NaCaLa_{0.8}(WO_4)_3$:$Ho_{0.2}$ were not detected. The strong 550-nm emission band in the green region corresponds to the $^5S_2/^5F_4 \rightarrow {}^5I_8$ transition, while the very strong emission 655-nm band in the red region corresponds to the $^5F_5 \rightarrow {}^5I_8$ transferred to the activator where radiation can be emitted. The Ho^{3+} ion activator is the luminescence center for these UC particles; the sensitizer Yb^{3+} enhances effectively the UC luminescence intensity because of the efficient energy transfer from Yb^{3+} to Ho^{3+}. The UC emissions are generated

by a two photon process through excited state absorption (ESA) and energy transfer (ET) [18, 19]. First, the Yb^{3+} ion sensitizer is excited from the $^2F_{7/2}$ level to the $^4F_{5/2}$ level under excitation of 980 nm pumping; it transfers its energy to the Ho^{3+} ions. Then the Ho^{3+} ions are populated from the $^5I_8$ ground state to $^5I_6$ excited state. This is a phonon-assisted energy transfer process because of the energy mismatch between the $^2F_{5/2}$ level of Yb^{3+} and the $^5I_6$ level of Ho^{3+}. Secondly, the Ho^{3+} in the $^5I_6$ level is excited to the $^5S_2$ or $^5F_4$ level by the same energy transfer from Yb^{3+}. In addition, the $^5S_2/^5F_4$ level of Ho^{3+} can also populated through excited state absorption. Finally, the green emission around 550 nm corresponding to the $^5S_2/^5F_4 \rightarrow {}^5I_8$ transition, takes place. For the red emission, the population of the $^5F_5$ level is generated by two different channels. One channel comes from the fact that Ho^{3+} in the $^5S_2/^5F_4$ level relaxes non-radiatively to the $^5F_5$ level. Another channel is closely related to the $^5I_7$ level populated by non-radiative relaxation from the $^5I_6$ excited state. The Ho^{3+} in the $^5I_7$ level is excited to the $^5F_5$ level by the energy transfer from Yb^{3+}. Therefore, the red emission around 655 nm corresponds to the $^5F_5 \rightarrow {}^5I_8$ transition [20- 21].

Fig. 4: Upconversion photoluminescence emission spectra of (a) $NaCaLa(WO_4)_3$, (b) $NaCaLa_{0.8}(WO_4)_3:Ho_{0.2}$, (c) $NaCaLa_{0.7}(WO_4)_3:Ho_{0.1}Yb_{0.2}$, and (d) $NacaLa_{0.5}(WO_4)_3:Ho_{0.05}Yb_{0.45}$ particles excited under 980 nm at room temperature.

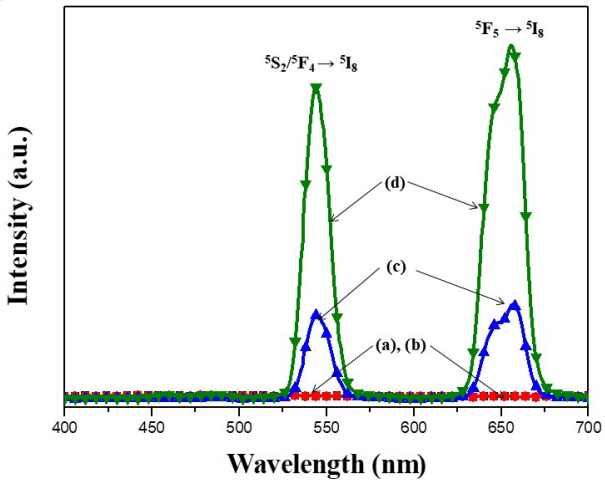

The logarithmic scale dependence of the UC emission intensities at 545 and 655 nm on the working pump power over the range of 20 to 110 mW in the $NaCaLa_{0.50}(WO_4)_2$: $Yb_{0.05}/Ho_{0.45}$ sample is shown in Fig. 5. In the UC process, the UC emission intensity is proportional to the slope value n of the irradiation pumping power, where n is the number of pumped photons required to produce UC emission [18]: $I \alpha P^n$ and $\mathrm{Ln}I \alpha n\mathrm{Ln}P$, where value n is the number of the pumped photons required to excite the upper emitting state, I is the UC luminescent intensity and P is the laser pumping power. As seen from Fig. 5, the calculated slope value n = 1.72 for green emission at 545 nm, and n = 1.83 for red emissions at 655 nm, respectively. These results show that the UC mechanism of green and red emissions can be explained by the multi-step energy transfer process in Ho^{3+}/Yb^{3+} co-doped phosphors [7-9, 22-25].

Fig. 5 : Logarithmic scale dependence of the UC emission intensity on the pump power in the range from 20 to 110 mW at 545 and 655 nm in the $NaCaLa_{0.50}(WO_4)_2$:$Ho_{0.02}$/$Yb_{0.45}$sample.

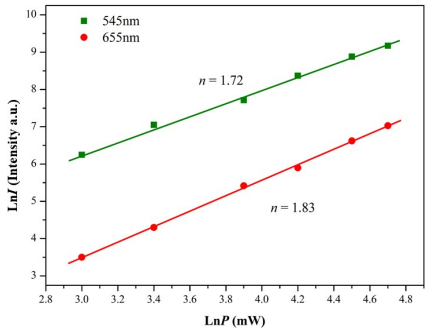

Fig. 6 shows the Raman spectra of the synthesized (a) $NaCaLa(WO_4)_3$, (b) $NaCaLa_{0.8}(WO_4)_3$: $Ho_{0.2}$, (c) $NaCaLa_{0.7}(WO_4)_3$: $Ho_{0.1}Yb_{0.2}$, and (d) $NaCaLa_{0.5}(WO_4)_3$: $Ho_{0.05}Yb_{0.45}$ particles excited by the 514.5-nm line of an Ar ion laser at 0.5 mW. The internal modes for the (a) $NaCaLa(WO_4)_3$ particles were detected at 200, 328, 388 and 915 cm^{-1}. The internal vibration mode frequencies are dependent on the lattice parameters and the degree of the partially covalent bond between the cation and the molecular ionic group $[WO_4]^{2-}$. The Raman spectra of the doped particles indicate the domination of strong peaks at higher frequencies of 833, 915, 1098, 1175 and 1268 cm^{-1}. The Raman spectra of the doped particles prove that the doping ions can influence the structure of the host materials. The combination of a heavy metal cation and the large inter-ionic distance for Ho^{3+} and Yb^{3+} substitutions in La^{3+} sites in the lattice result in a high probability of UC and phonon-splitting relaxation in $NaCaLa_{1-x}(WO_4)_3$ crystals. It might be induced by the structures of $NaCaLa_{1-x}(WO_4)_3$:Ho^{3+}/Yb^{3+} that were disordered by the incorporation of the Ho^{3+} and Yb^{3+} ions into the crystal lattice, which resulted in unit cell shrinkage accompanying the new phase formation. the $[WO_4]^{2-}$ group. The combination of a heavy metal cation and the large inter-ionic distance for the doped elements in La^{3+} sites in the lattice result in a high probability of UC and phonon-splitting relaxation in $NaCaLa_{1-x}(WO_4)_3$ crystals [23, 24].

Fig. 6: Raman spectra of the synthesized (a) $NaCaLa(WO_4)_3$, (b) $NaCaLa_{0.8}(WO_4)_3$:$Ho_{0.2}$, (c) $NaCaLa_{0.7}(WO_4)_3$:$Ho_{0.1}Yb_{0.2}$, and (d) $NaCaLa_{0.5}(WO_4)_3$:$Ho_{0.05}Yb_{0.45}$ particles excited by the 514.5-nm line of an Ar ion laser at 0.5 mW.

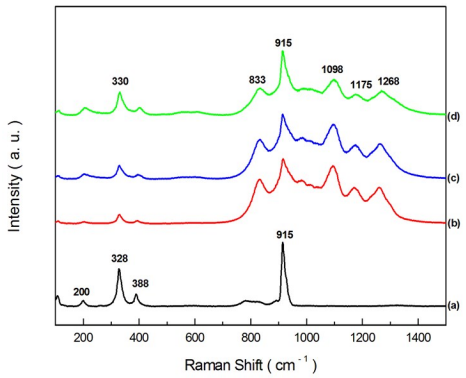

Conclusions

$NaCaLa_{1-x}(WO_4)_3:Ho^{3+}/Yb^{3+}$ yellow phosphors with doping concentrations of Ho^{3+} and Yb^{3+} (x = Ho^{3+} + Yb^{3+}, Ho^{3+} = 0.05, 0.1, 0.2 and Yb^{3+} = 0.2, 0.45) were successfully synthesized by the cyclic microwave-assisted sol-gel method. Well-crystallized particles formed after heat-treatment at 900°C for 16 h showed a fine and homogeneous morphology with particle sizes of 5-10 ìm. Under excitation at 980 nm, the UC intensities of $NaCaLa_{0.5}(WO_4)_3:Ho_{0.05}Yb_{0.45}$ particles exhibited yellow emissions based on a strong 545-nm emission band in the green region and a very strong 655-nm emission band in the red region; these emissions were assigned to the $^5S_2/^5F_4 \rightarrow {}^5I_8$ and $^5F_5 \rightarrow {}^5I_8$ transitions, respectively. The Raman spectra of the doped particles indicate the domination of strong peaks at higher frequencies of 833, 915, 1098, 1175 and 1268 cm^{-1}, which were induced by the structures of $NaCaLa_{1-x}(WO_4)_3:Ho^{3+}/Yb^{3+}$ that were disordered by the incorporation of the Ho^{3+} and Yb^{3+} ions into the crystal lattice. The high emitting efficiency of NCLW:Ho^{3+}/Yb^{3+} phosphors can be considered as potential applications of white emitting diodes in new optoelectronic devices.

Acknowledgment

This research was supported by the Basic Science Research Program through the National Research Foundation of Korea (NRF) funded by the Ministry of Science, ICT and future Planning (2018R1D1A1A09082321).

References

[1] M. Wang, G. Abbineni, A Clevenger, C. Mao, S. Xu, Nanomedicine: Nanotech. Biology, and Medicine, 7, 710 (2011).

[2] Y.J. Chen, H.M. Zhu, Y,F. Lin, X.H. Gong, Z.D. Luo, Y.D. Huang, Opt. Mat., 35, 1422 (2013).

[3] M. Lin, Y. Zho, S. Wang, M. Liu, Z. Duan, Y. Chen, F. Li, F. Xu, T. Lu, Bio. Adv., 30, 1551 (2012).

[4] L. Li, W. Zi, H. Yu, S. Gan, G. Ji, H. Zou, X. Xu, J. Lum., 143, 14 (2013).

[5] C.S. Lim, Ceramics International. 41, 2616 (2015).

[6] C.S. Lim, J. Physics and Chemistry of Solids,76, 65 (2015).

[7] J. Jin, K. Yang, J. Su, Z. Si, J. Lumin., 159, 178 (2015).

[8] Y. Xu, Y. Wang, L. Xing, X. Tan, 54, 50 (2013).

[9] D. Li, Y. Wang, X. Zhang, G.Shi, G. Liu, Y. Song, J. Alloys Compd., 550, 509 (2013).

[10] X. Liu, W. Xiang, F. Chen, W. Zhang, Z. Hu, Mater. Res. Bull., 47, 3417 (2012).

[11] X. Liu, W. Xiang, F. Chen, Z. Hu, W. Zhang, Mater. Res. Bull., 48, 281 (2013).

[12] N. Xue, X. Fan, Z. Wang, M. Wang, Mater. Lett., 61, 1576 (2007).

[13] S. Huang, D. Wang, Y. Wang, L. Wang, X. Zhang, P. Yang, J. Alloys Compd., 529, 140 (2012).

[14] J. Feng, J. Xu, Z. Zhu, Y. Wang, Z. You, J. Li, H. Wang, C. Tu, J. Alloys Compd., 566, 229 (2013).

[15] F. Song, L. Han, H. Tan, J. Su, J. Yang, J. Tian, G. Zhang, Z. Cheng, H. Chen, Opt. Comm., 259, 179 (2006).

[16] C.S. Lim, Mater. Res. Bull., 47, 4220 (2012).

[17] R. D. Shannon, Acta Cryst., A32, 751 (1976).

[18] H. Guo, N. Dong, M. Yin, W. Zhang, L. Lou, S. Xia, J. Phys. Chem. B, 108, 19205 (2004).

[19] Y. Xu, Y. Wang, L. Shi, L. Xing, X. Tan, Opt. Laser Tech., 54, 50 (2013).

[20] X. Li, Q. Nie, S. Dai, T. Xu, L. Lu, X. Zhang, J. Alloys Compd., 454, 510 (2008).

[21] L.G.A. Carvalho, L.A. Rocha, J.M.M. Buarque, R.R. Goncalves, C.S. Nascimento Jr., M.A. Schavon, S.J.L. Ribeiro, J.L. Ferrari, J. Lumin., 159, 223 (2015).

[22] H. Gong, D. Yqang, X. Zhao, E.Y.B. Pun, H. Lim, Opt. Mater., 32, 554 (2010).

[23] V.V. Atuchin, O.D. Chimitova, T.A. Gavrilova, M.S. Molokeev, Sung-Jin Kim, N.V. Surovtsev, B.G. Bazarov, J. Crys. Growth, 318, 683 (2011).

[24] V.V. Atuchin, O.D. Chimitova, S.V. Adichtchev, J.G. Bazarov, T.A. Gavrilova, M.S. Molokeev, N.V. Surovtsev, Zh.G. Bazarova, Mater. Lett., 106. 26 (2013).